Evolutionary Air-Conditioning Optimization Using an LSTM-Based Surrogate Evaluator

Yoshihiro Ohta
Mitsubishi Electric Corporation
5-1-1, Ofuna, Kamakura,
Kanagawa 247-8501 Japan,
Ota.Yoshihiro@dw.MitsubishiElectric.co.jp

Takafumi Sasakawa
Tokyo Denki University
Ishizaka, Hatoyama-machi,
Hiki-gun, Saitama 350-0394 Japan
sasa@rd.dendai.ac.jp

Hiroyuki Sato
The University of Electro-Communications
1-5-1 Chofugaoka, Chofu,
Tokyo 182-8585 Japan
h.sato@uec.ac.jp

***Abstract*—We propose a fast air-conditioning temperature optimization system using a surrogate solution evaluator. Simulation-based evolutionary optimization does not require the formulation of a mathematical model of the optimization problem and allows the treatment of the problem by considering a black box. However, the simulation-based solution evaluation is often time-consuming. Because evolutionary algorithms need to generate many candidate solutions for optimization, the time-consuming solution evaluation will be a bottleneck, which is encountered in air-conditioning temperature optimization. The building simulator provides the thermal comfort level and the power usage by inputting a candidate air-conditioning temperature setting through a complicated simulation. Although the results are useful compared with those obtained by a simple mathematical model, it is time-consuming. To accelerate the optimization process, we propose a surrogate evaluator based on the time-series predictive long short-term memory, which is a recurrent neural network architecture. Instead of the time-consuming building simulator, the surrogate evaluator outputs the two time-series data of the thermal comfort and power consumption, and schedules are optimized with the multi-objective particle swam-based optimizer OMOPSO. Experimental results show that the proposed system could obtain practical schedule sets, and the optimization was accelerated by using the surrogate evaluator.**

***Index Terms*—multi-objective optimization, surrogate solution evaluation, air-conditioning system**

I. Introduction

The reduction of energy consumption and carbon dioxide emission is essential for sustainable office building management. Owners of office buildings are required to achieve long-term energy reduction under regulations such as the Energy Performance of Buildings Directive in the EU [1], Energy Efficiency Resource Standard in the US [2], and Act on the Rational Use of Energy in Japan [3]. The air-conditioning system alone accounts for approximately 30 percent of the total power consumption in typical office buildings [4], [5]. The total power consumption of the air-conditioning system depends on its temperature setting, the outside air temperature, room usage, and other variable disturbances. The control of air-conditioning can significantly contribute to the reduction of power consumption, and concern over optimal air-conditioning control in office buildings has been increasing. Building managers develop power consumption plans based on historical power consumption data of their buildings with the goal of not exceeding the set power consumption limit. When the power consumption is likely to exceed the limit, the building manager modifies the original plan to satisfy the target power consumption, introducing measures such as controlling the temperature setting and reducing the number of heat source units. However, this deteriorates the thermal comfort of office workers. It has been reported that power savings, which are accompanied by comfort deterioration, are less economically effective overall, because a lower thermal comfort affects the productivity of the office workers [6], [7]. Therefore, it is desirable to reduce the power consumption without compromising the thermal comfort of the office workers.

For the optimization of the air-conditioning schedule, mathematical programming techniques and evolutionary algorithms have been employed so far [8]–[10]. For example, a multi-objective air-conditioning optimization, which searches a solution set to optimize the power consumption and the thermal comfort simultaneously, has been proposed [11]. In our previous work, we proposed an evolutionary multi-objective air-conditioning schedule optimization algorithm [12]. Our system dynamically changes the temperature setting every hour while most of the conventional systems employ a fixed temperature setting for a whole day. The solution to be optimized is a time-series temperature setting and can be input into the building ' s energy simulator EnergyPlus [13], which is widely used in the construction industry. The simulator outputs the thermal comfort level and the power consumption of the solution as multiple objective values. Based on these objective values, in this study, we improve the time-series temperature settings by using an evolutionary algorithm. Our previous work showed that the system could obtain temperature settings better than conventional fixed temperature settings in terms of both power consumption and human comfort level.

The simulator-based evolutionary optimization does not require the development of a mathematical model of objective functions and allows the treatment of the optimization problem by considering a black box. However, it requires high computational power to evaluate a solution. The simulator-based air-conditioning optimization system [12] is no exception, and the evaluation of a solution using the EnergyPlus simulation evaluator is computationally expensive. Because this system obtains a daily temperature schedule in a single run, we repeat to run the system for tomorrow every day. As the

978-1-7281-6929-3/20/$31.00 ©2020 IEEE

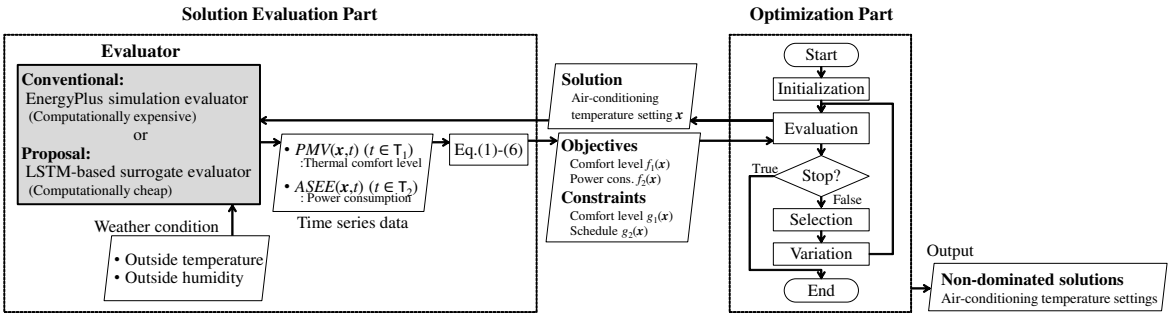

Fig. 1. Air-conditioning temperature schedule optimization system

evaluation of each solution evaluation is time-consuming, and the optimization time is limited to one day, the number of solution evaluation runs must be decreased. Therefore, we may not obtain an accurate result by evolutionary optimization.

In this work, we aim at accelerating the evolutionary air-conditioning optimization by using a surrogate solution evaluator. We construct a surrogate evaluator that predicts the two time-series data of the thermal comfort level and the power consumption instead of using the time-consuming EnergyPlus simulator. To predict the two time-series data of the thermal comfort level and the power consumption, the surrogate evaluator employs the long short-term memory (LSTM), which is a recurrent neural network (RNN) architecture. For the optimization, we use OMOPSO, which is a particle swarm-based optimizer for multi-objective continuous optimization. Through computational experiments, we discuss the accuracy of the LSTM-based surrogate evaluator, the optimized result, its quality, and the optimization time.

II. Overview of the Air-Conditioning Temperature Optimization System

Fig. 1 show a process flow diagram of the air-conditioning optimization systems. The left side of this figure shows the solution evaluation part, and the right side shows the optimization part. The two parts communicate by using the air-conditioning temperature setting and its objective and constraint values. The outputs of this system are optimized air-conditioning temperature schedules shown on the rightmost side. Note that the evaluator is in the solution evaluation part, which is the gray rectangle in the figure. The conventional system [12] used the EnergyPlus simulation evaluator, which is computationally expensive because it simulates additional data that are not required. On the other hand, the proposed system uses a surrogate evaluator that imitated the EnergyPlus simulation and is computationally cheap. For both evaluators, inputs are time-series air-conditioning temperature settings in a day and the weather conditions. Outputs are two-kinds of time-series data on the day. One is the predicted mean vote (PMV) index value [14], [15], which is related to the human thermal comfort, and the other is the air system electric energy (ASEE) value, which is related to the power consumption.

III. Simulation-Based Solution Evaluator

In this section, we describe the EnergyPlus simulation shown in Fig. 1, which is the solution evaluator used in the conventional air-conditioning optimization system [12].

A. Building Model

Fig. 2 shows the target office building model considered in this study. The building considered has eight floors above the ground, and the total area of the floors is 11,781 $[m^2]$. The building has office rooms on every floor, and a central air-conditioning system with a water-cooled centrifugal chiller with a coefficient of performance (COP) of 5.96 is employed as the heat source machine. The air-conditioning system supplies cooled and heated air through the air handling unit (AHU) and the variable air volume (VAV) unit to each floor. The other specifications of the building are the same as in [12].

We constructed the building model by using the EnergyPlus building energy simulator [13], which is widely used in the construction industry to precisely simulates the air movement in the building. However, the simulation is computationally expensive because it simulates additional data that are not useful in some cases. In the air-conditioning optimization system, we use the two time-series data of the human thermal comfort level and power consumption from the simulation results.

B. Input

Because weather conditions affect the simulation results, as shown in Fig. 1, the evaluator needs two time-series data of the outdoor temperature and the outdoor humidity, which are obtained from weather forecast data. Furthermore, we input a time-series air-conditioning temperature setting. This system optimizes an hourly time-series air-conditioning temperature setting and dynamically changes the temperature settings during the day, unlike most of the conventional systems, which use a constant temperature setting throughout the day.

The temperature setting is represented as the design variable vector $\boldsymbol{x}$. Each element x_t is a setting temperature at a setting time $t \in \mathcal{T}_{set}$, where $\mathcal{T}_{set}$ is a set of setting time. Because our target is an office building, the time period to be optimized is set to 5:00–23:00. Therefore, the design variable vector is $\boldsymbol{x} = (x_{5:00}, x_{6:00}, \ldots, x_{23:00})$, and it has $n = 19$ elements.

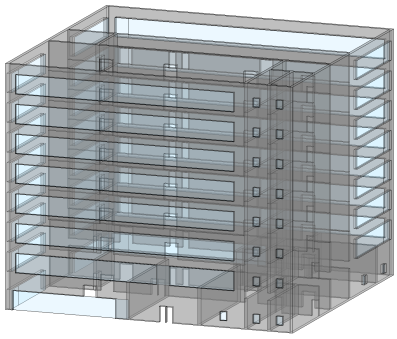

Fig. 2. Appearance of target office building model

The temperature setting has the lower limit x^{min} and the upper limit x^{max}, i.e., $x^{min} \leq x_t \leq x^{max}$ $(t \in \mathcal{T}_{set})$. In this work, the same temperature setting schedule $\boldsymbol{x}$ is applied to all rooms in the building.

C. Output

As shown in Fig. 1, the outputs of the evaluator are two time-series data.

The first one is a time-series PMV [14], [15] related to the human thermal comfort in the building. The PMV evaluates the average thermal sensation of the people in the indoor space by using the dry-bulb temperature, relative humidity, wind speed, mean radiation temperature (MRT), metabolic rate, and number of clothes. The value range of the PMV is between -3 (cold) and +3 (hot). A PMV of zero corresponds to the most comfortable environment, and a PMV with a large absolute value corresponds to an uncomfortable environment. For an air-conditioning temperature schedule $\boldsymbol{x}$, the EnergyPlus simulator outputs a time-series PMV every hour within the possible working time between 7:00 and 22:00. Specifically, the first time-series outputs are $PMV(\boldsymbol{x}, t)$ $(t \in \mathcal{T}_1 = \{7:00, 8:00, ..., 21:00, 22:00\})$.

The second one is a time-series ASEE value, which is the electric power consumed [J]. For an air-conditioning temperature schedule $\boldsymbol{x}$, the EnergyPlus simulator outputs time-series ASEE values every hour between 0:00 and 24:00. Specifically, the second time-series outputs are $ASEE(\boldsymbol{x}, t)$ $(t \in \mathcal{T}_2 = \{0:00, 1:00, \ldots, 23:00, 24:00\})$.

D. Objectives and Constraints

This system has two objectives to be optimized.

The first objective, the human thermal comfort level, is formulated as the aggregation of the time-series PMVs output by the evaluator as follows:

$$\text{Minimize} \quad f_1(\boldsymbol{x}) = \frac{1}{|\mathcal{T}_1|} \sum_{t \in \mathcal{T}_1} |PMV(\boldsymbol{x}, t)|, \qquad (1)$$

where $PMV(\boldsymbol{x}, t)$ is the PMV of the air-conditioning system at time t.

The second objective, the power consumption, is formulated as the aggregation of the time-series $ASEE$ values output by the evaluator as follows:

$$\text{Minimize} \quad f_2(\boldsymbol{x}) = \sum_{t \in \mathcal{T}_2} ASEE(\boldsymbol{x}, t) \quad , \qquad (2)$$

where $ASEE(\boldsymbol{x}, t)$ is the electric power consumption [J] of the air-conditioning system at time t.

Moreover, this system has two constraints to satisfy.

The first is related to the PMVs. A PMV range of $[-0.5, +0.5]$ is recommended by ISO to obtain a comfortable environment. To avoid an excessively uncomfortable environment with a large PMV, we introduce the first constraint on the PMV. A feasible schedule $\boldsymbol{x}$ is

$$\text{Subject to} \quad g_{1,t}(\boldsymbol{x}) = |PMV(\boldsymbol{x}, t)| \leq 0.5 \quad (\forall t \in \mathcal{T}_1). \quad (3)$$

Solutions satisfying the above constraint for all times $t \in \mathcal{T}_1$ are feasible, and solutions that do not satisfying every one of them are infeasible. The first constraint violation value is formulated as follows:

$$v_1(\boldsymbol{x}) = \sum_{t \in \mathcal{T}_1} \max\{0, g_{1,t}(\boldsymbol{x}) - 0.5\}. \qquad (4)$$

The second constraint is related to a dynamic change in the temperature setting. To avoid a rapid increase in the power consumption due to drastic changes in the air-conditioning temperature setting, the maximum difference in the temperatures between two consecutive hours is limited to 2.0 [°C]. We introduce the second constraint on the dynamic change of the air-conditioning temperature. Feasible schedule $\boldsymbol{x}$ is

$$\text{Subject to} \quad g_{2,t}(\boldsymbol{x}) = |x_t - x_{t-1:00}| \leq 2.0 \quad (\forall t \in \mathcal{T}_{set} \backslash 5:00). \quad (5)$$

Solutions satisfying the above constraint condition at all times $t \in \mathcal{T}_{set}$ except the first time $(t = 5:00)$ are feasible, and solutions that do not satisfy every one of them are infeasible. The second constraint violation value is formulated as follows:

$$v_2(\boldsymbol{x}) = \sum_{t \in \mathcal{T}_{set}} \max\{0, g_{2,t}(\boldsymbol{x}) - 2.0\} \qquad (6)$$

IV. Proposal: LSTM-Based Surrogate Evaluator

In this section, we describe the LSTM-based surrogate evaluator shown in Fig. 1, which is the solution evaluator in the proposed air-conditioning optimization system. The EnergyPlus simulation evaluator in the conventional system is replaced by the LSTM-based surrogate evaluator in the proposed system.

A. Overview

For each air-temperature setting schedule $\boldsymbol{x}$, the conventional system obtains the two time-series data of the thermal comfort level $PMV(\boldsymbol{x}, t)$ and the power consumption $ASEE(\boldsymbol{x}, t)$ by using the EnergyPlus simulation evaluator. Then, the two objective values $f_1(\boldsymbol{x})$ and $f_2(\boldsymbol{x})$ are calculated from the two time-series data. However, the EnergyPlus based

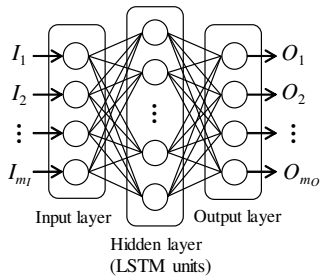

Fig. 3. Overall structure of the LSTM-based surrogate evaluator

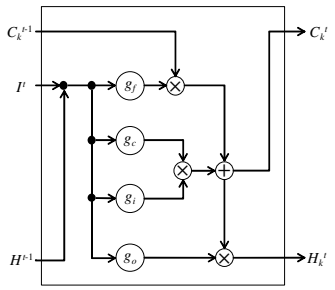

Fig. 4. LSTM unit used in the proposed system

simulation is computationally expensive because the evolutionary algorithm generates many candidate schedules during the optimization process.

The proposed system replaces the time-consuming EnergyPlus simulation evaluator with a computationally cheap surrogate evaluator. The surrogate evaluator outputs the thermal comfort level $PMV(\boldsymbol{x}, t)$ and the power consumption $ASEE(\boldsymbol{x}, t)$ by inputting the air-temperature setting schedule $\boldsymbol{x}$. Then, the proposed system calculates the two objective values $f_1(\boldsymbol{x})$ and $f_2(\boldsymbol{x})$ from the two time-series data obtained by the surrogate evaluator. Thus, the proposed system accelerates the air-conditioning temperature optimization by replacing the time-consuming EnergyPlus simulation with the computationally cheap surrogate evaluator.

B. LSTM-Based Surrogate Evaluator

In this work, to build the surrogate evaluator to obtain the two time-series data of the thermal comfort level and the power consumption, we utilize the LSTM, which is one of the RNNs [16]. The LSTM, which includes a memory cell, receives state inputs of the previous time-steps and maintains and utilizes the previous states with input, forget, and output gates to forecast the next incoming data. It has been known that LSTM is one of the promising ways to learn time-series and has successfully been applied to real-world problems, such as natural language processing [17].

Fig. 3 shows the neural network structure of the surrogate evaluator used in the proposed system. Here, I_i $(i = 1, 2, \ldots, m_I)$ and O_j $(j = 1, 2, \ldots, m_O)$ are input and output values, respectively, m_I is the number of input values and units in the input layer, and m_O is the number of output values and units in the output layer. The hidden layer between the input and output layers is the LSTM layer, and all units in the LSTM layer are fully connected to all units in the input and output layers. The number of units in the LSTM layer is m_H.

Fig. 4 shows the LSTM unit structure used in this work, which was employed from [16]. The figure represents k-th LSTM units. Here, I^t, H_k^t, and C_k^t are the input vector to the LSTM layer, the state of the k-th LSTM unit, and the state of the memory cell in the k-th LSTM unit at time step t, respectively; g_f is the forget gate, g_c is the memory cell gate, g_i is the input gate, and g_o is the output gate. The output value on each gate in the k-th unit at time step t is calculated by

$$O_k^{Gt} = f^G\left(\sum_{i=1}^{m_I} w_{ki}^G \cdot I_i^t + \sum_{h=1}^{m_H} u_{kh}^G \cdot H_h^{t-1} + \theta_k^G\right) \quad (k = 1, 2, \ldots, m_H), \tag{7}$$

where G is the gate type (g_f, g_c, g_i, or g_o), w is the weight value for the input I^t, u is the weight value for the previous state of the LSTM unit H^{t-1}, θ is the bias term, and f^G is the activation function for the gate G. For the activation function f^{g_c}, we employed the hyperbolic tangent function. For the other gates, we employed the sigmoid function as the activation function. The state of memory cell C_k^t is calculated by

$$C_k^t = O_k^{g_i t} \cdot O_k^{g_c t} + O_k^{g_f t} \cdot C_k^{t-1}. \tag{8}$$

Then, the state of the k-th LSTM unit H_k^t is calculated by

$$H_k^t = O_k^{g_o t} \cdot \tanh(C_k^t). \tag{9}$$

The output value on each unit in the output layer is calculated by

$$O_j = f_O\left(\sum_{k=1}^{m_H} w_k \cdot H_k + \theta_j\right) \quad (j = 1, 2, \ldots, m_O), \tag{10}$$

where H_k is the output of the k-th unit in the LSTM layer, w_k is its weight coefficient, θ_j is the bias term to the j-th output unit, and f_O is the activation function.

C. Input and Output

For the network shown in Fig. 3, we input air-temperature setting x_t at time-step t and obtain two time-series data of the thermal comfort level $PMV(\boldsymbol{x}, t)$ and the power consumption $ASEE(\boldsymbol{x}, t)$ as outputs. Because these outputs are affected by the weather conditions, we also input the outdoor temperature and outdoor humidity.

Note that the input of Fig. 3 is data only at time-step t and the output of Fig. 3 is its result. Therefore, to obtain time-series outputs, we repetitively input time-series input data to the network of Fig. 3. During the repetition, the LSTM units shown in Fig. 4 maintain the previous states.

In the proposed system, the total number of input values and units is $m_I = 3$, I_1 is the air-temperature setting x_t at timestep t, I_2 is the outdoor temperature, and I_3 is the outdoor humidity. The total number of output values and units is $m_o = 2$, O_1

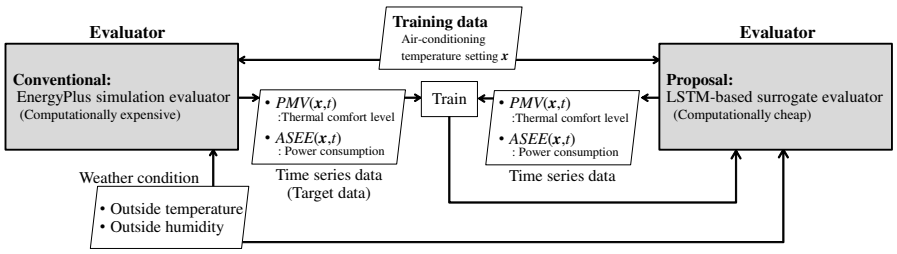

Fig. 5. Training of the LSTM-based surrogate evaluator

is thermal comfort level $PMV(\boldsymbol{x}, t)$, and O_2 is the power consumption $ASEE(\boldsymbol{x}, t)$.

D. Training

We trained the LSTM-based surrogate evaluator with seven-day training data. Fig. 5 shows the process flow diagram of the training process. As input data, we randomly generated air-conditioning temperature settings to satisfy the second constraint and used the actual outdoor temperature and humidity from the weather records matched to the target period. To obtain target data, we used the EnergyPlus simulator with the training input data.

V. Evolutionary Optimization

A. Particle Swarm-Based Multi-Objective Optimization

For the optimization with the proposed LSTM-based surrogate evaluator, we use the particle swarm-based multi-objective optimizer OMOPSO [18], which is a promising evolutionary algorithm for solving multi-objective continuous optimization problems. Our previous system [12], [19] also employed this algorithm. This section briefly introduces the OMOPSO algorithm.

Step 1: Initialize the particles (schedules) $\mathcal{P}$ as random real value vectors, the archive set $\mathcal{A}$ as the empty set, and the generation counter as $g = 1$.

Step 2: Evaluate each particle $\boldsymbol{x}^g \in \mathcal{P}$ by using the evaluator, obtain objective values of the thermal comfort level f_1, the power consumption f_2, and two constraint violation values v_1 and v_2, and set them as the personal best $\boldsymbol{x}_{pbest}$.

Step 3: Perform the non-dominated sorting to the combined set $\mathcal{P} \cup \mathcal{A}$. Update both the archive particle set $\mathcal{A}$ and the leader particle set $\mathcal{L}$ with the top non-dominated particles in the combined set $\mathcal{P} \cup \mathcal{A}$.

Step 4: Update the velocity and position of each particle in $\mathcal{P}$ by

$$\boldsymbol{v}^{g+1} = w \cdot \boldsymbol{v}^g + c_1 \cdot r_1(\boldsymbol{x}_{pbest} - \boldsymbol{x}^g) + c_2 \cdot r_2(\boldsymbol{x}_{gbest} - \boldsymbol{x}^g) \quad (11)$$

$$\boldsymbol{x}^{g+1} = \boldsymbol{x}^g + \boldsymbol{v}^{g+1}, \quad (12)$$

where $\boldsymbol{v}^g$ is the velocity of the particle; $\boldsymbol{x}^g$ is the position of the particle in the continuous variable space at the g-th generation; w, c_1, and c_2 are user-defined weight values; and r_1 and r_2 are uniform random values in $[0, 1)$. Position $\boldsymbol{x}_{pbest}$ is the best position of the particle found so far, and $\boldsymbol{x}_{gbest}$ is the position of a particle selected from $\mathcal{L}$ based on the binary tournament selection. When the updated variable $\boldsymbol{x}^{g+1}$ exceeds the variable value range $[x^{min}, x^{max}]$, it is returned on the boundary, and its velocity $\boldsymbol{v}^{g+1}$ is multiplied by -1.

Step 5: Divide $\mathcal{P}$ into three particle sets: $\mathcal{Q}$, $\mathcal{R}$, and $\mathcal{S}$.

Step 6: Perform the uniform mutation to particles in $\mathcal{R}$, and the non-uniform mutation to particles in $\mathcal{S}$. No mutation is applied to particles in $\mathcal{Q}$. The uniform mutation adds uniform random values in $[-0.25(x^{max} - x^{min}), 0.25(x^{max} - x^{min}))$ for each variable with a mutation probability p_m. The non-uniform mutation changes the mutation range at every generation for each variable with a mutation probability p_m [20]. In this work, its range is as follows:

$$x_i'^{g+1} = \begin{cases} x_i^{g+1} + \Delta(g, x^{max} - x_i^{g+1}), \text{if } r_3 < 0.5 \\ x_i^{g+1} - \Delta(g, x_i^{g+1} - x^{min}), \text{otherwise,} \end{cases} \quad (13)$$

where $x_i'^{g+1}$ is the i-th element of the design variable vector $\boldsymbol{x}'^{g+1}$, g^{max} is the total number of generations, and r_3 is a uniform random value in $[0, 1)$; $\Delta(g, y)$ is the range of variation and is calculated by

$$\Delta(g, y) = y \cdot \left(1 - r_4^{\left(1 - \frac{g}{g^{max}}\right)^b}\right), \quad (14)$$

where r_4 is a uniform random value in $[0, 1)$, b is a parameter used to adjust the range of variation. When the mutated variable exceeds the range $[x^{min}, x^{max}]$, it is returned on the boundary.

Step 7: Combine the three particle sets $\mathcal{Q}$, $\mathcal{R}$, and $\mathcal{S}$ to make the new particle set $\mathcal{P}$ (=$\mathcal{Q} \cup \mathcal{R} \cup \mathcal{S}$).

Step 8: Evaluate each particle in $\mathcal{P}$ with the evaluator and obtain objective values and constraint violation values. When each particle constrain-dominates [21] its personal best $\boldsymbol{x}_{pbest}$, update it with the current particle.

Step 9: Perform the non-dominated sorting to the combined set $\mathcal{P} \cup \mathcal{A}$. Update the leader particle set $\mathcal{L}$ with the top non-dominated particles in the combined set $\mathcal{P} \cup \mathcal{A}$. In the same way, update the archive particle set $\mathcal{A}$ with the top non-dominated particles in the combined set $\mathcal{P} \cup \mathcal{A}$. When the size of the leader particle $\mathcal{L}$ exceeds its limit $N^{\mathcal{L}}$, maintain only the top $N^{\mathcal{L}}$ particles based on the crowding distance [21].

TABLE I
LEARNING PARAMETERS OF THE LSTM NETWORK

Parameter	Value
Minibatch size	200
Number of train	2000
Unit size of LSTM layer m_h	250
Optimization method	Adam
Learning rate α	0.001
Gradient decay rate β_1	0.9
Squared gradient decay rate β_2	0.999

TABLE II
PARAMETERS OF THE OMOPSO

Parameter	Value
Number of base particles $\|\mathcal{P}\|$	35
Number of leader particles $\|\mathcal{L}\|$	100
Number of archived particles $\|\mathcal{A}\|$	Unlimited
ϵ	0.0075
Number of generations g^{max}	500
Number of variables n	19
Mutation probability p_m	$1/n$
Coefficient of non-uniform mutation b	5 [20]
Weight w	Uniform random values in [0.1, 0.5)
Weight c_1, c_2	Uniform random values in [1.5, 2.0)

Step 10: If the generation counter g meets the termination condition g^{max}, output the archive particle set $\mathcal{A}$ as the optimization result. Otherwise, increment the generation counter g and go to **Step 4**.

VI. EXPERIMENTAL SETTINGS

A. Experiments

First, we confirm the accuracy of the proposed LSTM-based surrogate evaluator by comparing the outputs of the LSTM-based surrogate evaluator and the conventional EnergyPlus simulation evaluator for the same input. Next, we perform the proposed air-conditioning schedule optimization with the LSTM-based surrogate evaluator and discuss its results.

B. Building

As weather condition data, we use the expanded automated meteorological data acquisition system (AMeDAS) records [22] from Tokyo, Japan. The air-conditioning is set to cooling mode, the lower limit of the temperature is set to $x^{min} = 18$ [°C], and the upper limit is set to $x^{max} = 30$ [°C]. We assume that the occupancy of the office workers, and the usage of lightings and equipment in the office rooms are the same as those in [12].

C. Learning

Table I shows the learning parameters set to obtain the LSTM network used in the proposed system. To evaluate the prediction error, we employed the mean squared error (MSE). The value ranges of input and output data were normalized to [0,1]. We use the LSTM-based surrogate evaluator implemented by the programming language Python on a computer with Windows 10 (64 bit), Intel Core i7-3770K (3.5 GHz), and 16 GB RAM.

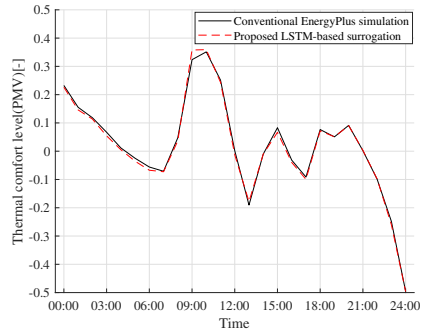

(a) Thermal comfort level (PMV)

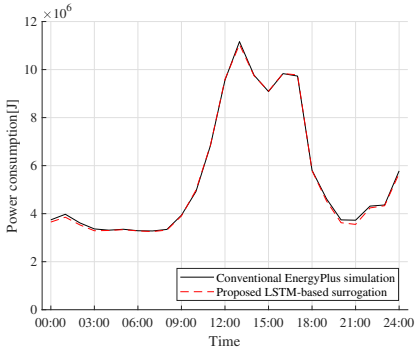

(b) Power consumption

Fig. 6. Time-series outputs of the EnergyPlus simulation evaluator and the proposed LSTM-based surrogate evaluator

D. Optimization

Table II shows the parameters of the OMOPSO used in our proposed system. For weight and random values, we employ the same setting used in [18]. We implement the OMOPSO by the programming language Java on the computer described above. To reduce the optimization time, the particle (schedules) evaluations are parallelized into eight threads at the same time.

VII. EXPERIMENTAL RESULTS AND DISCUSSION

A. Accuracy of Proposed LSTM-based Surrogate Evaluator

First, we verify the accuracy of the proposed LSTM-based surrogate evaluator. We trained the LSTM-based surrogate evaluator with the training data mentioned above and checked the error between the true values and the output values of the surrogate evaluator by using the validation data.

Fig. 6 shows the two time-series data of the thermal comfort level and the power consumption obtained by the EnergyPlus simulation evaluator and the LSTM-based surrogate evaluator for a one-day time-series validation data.

We see that two errors are sufficiently small because the error on the power consumption is approximately 1%, and the error on the thermal comfort level is lower than 1% in its possible value range $[-3, 3]$. Furthermore, we see that the values obtained by the proposed LSTM-based surrogate evaluator could estimate the hourly transitions of these values. These results confirm the validity of the proposed LSTM-based evaluator as a surrogate model of the EnergyPlus simulator.

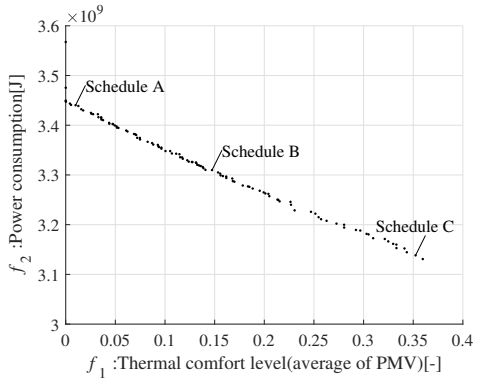

Fig. 7. Thermal comfort and power consumption of temperature setting schedules obtained by the OMOPSO optimizer using the proposed LSTM-based surrogate evaluator

B. Schedules Obtained by Multi-Objective Optimization

Fig. 7 shows all solutions (air-conditioning schedules) obtained by the proposed system using the LSTM-based surrogate evaluator at the final generation. The horizontal and vertical axes indicate the thermal comfort index and power consumption of the air-conditioning system to be minimized, respectively. Each point indicates the objective values of an air-conditioning temperature schedule, which are the time-series temperature settings in one day. From the results, we see that the proposed system could obtain solutions that approximate the trade-off between thermal comfort and power consumption in the air-conditioning system of the target building. A comfortable temperature setting with a small f_1 compromises the power consumption f_2 to operate the air-conditioning system, and an eco-friendly temperature setting with a small f_2 sacrifices the environmental comfort f_1 of office workers in the building.

Next, we observe the time-series data of schedules obtained by the proposed system. For each of three schedules A, B, and C in Fig. 7, its time-series data of the temperature setting, thermal comfort as PMV index, and power consumption are shown in Fig. 8. The figures of the thermal comfort and power consumption show the outputs of both the proposed LSTM-based surrogate evaluator and the EnergyPlus simulation evaluator.

The results show that the thermal comfort levels are within $[-0.5, -0.5]$, and feasible schedules satisfying the minimum comfort level $g_{1,t}$ could be obtained. Furthermore, the temperature setting changes between two consecutive hours are less than 2.0 [°C], and feasible schedules satisfying $g_{2,t}$ could also be obtained. As shown in Fig. 6, in the case of schedule A, the difference between the two outputs of the proposed LSTM-based surrogate evaluator and the EnergyPlus simulation evaluator is relatively small. Because the proposed surrogate evaluation is accurate, we can accelerate the evolutionary optimization by using the proposed LSTM-based surrogate evaluator instead of using a time-consuming EnergyPlus simulation evaluator. However, the difference is larger in schedules B and C because the training data for the LSTM are not enough for these cases. We can expect to decrease the difference and improve the accuracy of the surrogate evaluator by including training data with PMVs close to 0.5, which corresponds to the border of the thermal comfort constraint $g_{1,t}$, or through concurrent learning of the LSTM model during the evolutionary air-conditioning optimization. Because the optimization system may face unexpected situations, it will be effective for the EnergyPlus simulation evaluator for some schedules and updating the LSTM-model during the optimization, while the LSTM-based surrogate evaluates most of the schedules.

We also confirmed that the proposed LSTM-based surrogate evaluator could obtain feasible and useful temperature settings in this experiment.

TABLE III
COMPUTATIONAL TIME COMPARISON

	Conventional system (EnergyPlus simulation)	Proposed system (LSTM-based surrogate)
One evaluation time	37.3 [seconds]	2.79 [seconds]
Optimization time	23.4 [hours]	2.77 [hours]

C. Computational Time

Table III shows the average evaluation time of one schedule and the total computational time of the optimization. From the results, we see that the evaluation of one schedule with the proposed LSTM-based surrogate evaluator is approximately 13 times faster than that with the conventional EnergyPlus simulation evaluator. Furthermore, the total optimization time of the proposed system is 2.77 h, which is 1/8 of that with the conventional system. Thus, the proposed system could accelerate the evolutionary optimization of the air-conditioning schedule settings.

The acceleration achieved by the proposed surrogate evaluator allows us to use more generations and a large population to improve the schedule quality further. Furthermore, to obtain a one-day air-conditioning schedule, the conventional system needed almost a day, so we needed to execute the system one day before. However, the accuracy of the weather forecast data of the outdoor temperatures and the outdoor humidity is improved during the day, improving the optimization result. Therefore, it is desirable to use their forecasts just before the operation of the air-conditioning schedule. The acceleration of schedule evaluation by the proposed surrogate evaluator not only speeds up the optimization but also improves the schedule quality by using highly accurate weather condition data.

VIII. CONCLUSIONS

To accelerate the air-conditioning temperature optimization, we proposed a surrogate evaluator based on the time-series predictive LSTM. The LSTM-based surrogate evaluator outputs the two time-series data of the thermal comfort and the power consumption instead of the time-consuming EnergyPlus simulation evaluator, and the schedules are optimized with the OMOPSO based on the objective values calculated by the obtained two time-series data. Experimental results showed

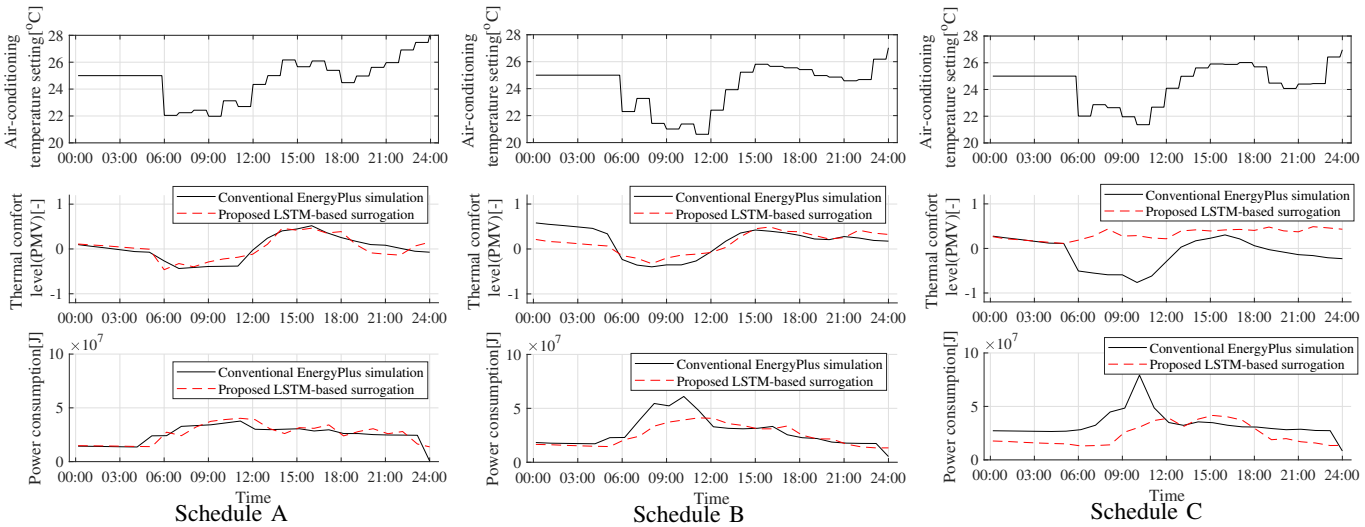

Fig. 8. Time series data of schedules obtained by the OMOPSO optimizer

that the proposed system using the LSTM-based surrogate evaluator obtained the non-dominated practical schedule set showing the tradeoff between the thermal comfort level and the power consumption. Furthermore, we showed that the air-conditioning temperature optimization was accelerated by using the surrogate evaluator. The proposed surrogate evaluator speeds up the optimization and improves the quality of the obtained schedule by using high accurate weather forecasts of the outdoor temperature and humidity.

As future works, we are building a concurrent learning method using an LSTM-based evaluator during evolutionary optimization. We are also designing an efficient evolutionary search method that can obtain quality schedules with fewer schedule evaluations using the surrogate model.

REFERENCES

[1] European Commission. (2016) amending Directive 2010/31/EU on the energy performance of buildings. http://eur-lex.europa.eu/legal-content/EN/TXT/HTML/?uri=CELEX:52016SC0414. Visited on Jan. 4, 2019.

[2] American Council for an Energy-Efficient Economy. (2017) Energy Efficiency Resource Standard (EERS). http://aceee.org/topics/energy-efficiency-resource-standard-eers. Visited on Jan. 4, 2019.

[3] Ministry of Internal Affairs and Communications. (2009) Act on the Rational Use of Energy. http://www.japaneselawtranslation.go.jp/law/detail/?vm=04&re=02&id=1855&lvm=02. Visited on Jan. 4, 2019.

[4] U. S. Energy Information Administration, *Annual Energy Outlook 2017*, 2017.

[5] Japanese Agency for Natural Resources and Energy, *FY2016 Annual Report on Energy*, 2017.

[6] R. Fabius, R. D. Thayer, D. L. Konicki, C. M. Yarborough, K. W. Peterson, F. Isaac, R. R. Loeppke, B. S. Eisenberg, and M. Dreger, "The Link Between Workforce Health and Safety and the Health of the Bottom Line: Tracking Market Performance of Companies That Nurture a Culture of Health," *Journal of Occupational and Environmental Medicine*, vol. 55, no. 9, pp. 993–1000, 2013.

[7] World Green Building Council. (2014) Health, Wellbeing and Productivity in Offices: The Next Chapter for Green Building. http://www.worldgbc.org/news-media/health-wellbeing-and-productivity-offices-next-chapter-green-building. Visited on Jan. 4, 2019.

[8] J. Xiao, J. Xie, X. Chen, K. Yu, Z. Chen, and Z. Li, "Energy Cost Reduction Robust Optimization for Meeting Scheduling in Smart Commercial buildings," in *2017 IEEE Conference on Energy Internet and Energy System Integration (EI2)*, Nov 2017, pp. 1–5.

[9] M. Alhaider and L. Fan, "Mixed Integer Programming for HVACs Operation," in *2015 IEEE Power Energy Society General Meeting*, July 2015, pp. 1–5.

[10] Y. Xu, K. Ji, Y. Lu, Y. Yu, and W. Liu, "Optimal Building Energy Management using Intelligent Optimization," in *2013 IEEE International Conference on Automation Science and Engineering (CASE)*, Aug 2013, pp. 95–99.

[11] Y. Zhang, P. Zeng, and C. Zang, "Multi-objective Optimal Control Algorithm for HVAC Based on Particle Swarm Optimization," in *Fifth International Conference on Intelligent Control and Information Processing*, Aug 2014, pp. 417–423.

[12] Y. Ohta and H. Sato, "Evolutionary Multi-objective Air-conditioning Schedule Optimization for Office Buildings," in *Proceedings of the Genetic and Evolutionary Computation Conference Companion*, ser. GECCO '18. ACM, 2018, pp. 296–297.

[13] National Renewable Energy Laboratory. EnergyPlus. https://energyplus.net/. Visited on Jan. 4, 2019.

[14] International Organization for Standardization, *ISO 7730:2005 Ergonomics of the thermal environment – Analytical determination and interpretation of thermal comfort using calculation of the PMV and PPD indices and local thermal comfort criteria*, 2005.

[15] P. O. Fanger, *Thermal Comfort*. McGraw-Hill Book Company, 1973.

[16] F. A. Gers, J. Schmidhuber, and F. Cummins, "Learning to Forget: Continual Prediction with LSTM," *Neural Computation*, vol. 12, no. 10, pp. 2451–2471, Oct 2000.

[17] I. Sutskever, O. Vinyals, and Q. Le, "Sequence to Sequence Learning with Neural Networks," *Advances in NIPS*, 2014.

[18] M. R. Sierra and C. A. C. Coello, "Improving PSO-Based Multi-objective Optimization Using Crowding, Mutation and ϵ-Dominance," in *Evolutionary Multi-Criterion Optimization*. Berlin, Heidelberg: Springer, 2005, pp. 505–519.

[19] Y. Ohta and H. Sato, "Evolutionary Optimization of Air-conditioning Schedule Robust for Temperature Forecast Errors," in *2019 IEEE Congress on Evolutionary Computation (CEC)*, June 2019, pp. 2482–2489.

[20] S. C. Esquivel and C. A. C. Coello, "On the Use of Particle Swarm Optimization with Multimodal Functions," in *The 2003 Congress on Evolutionary Computation, (CEC '03)*, vol. 2, 2003, pp. 1130–1136.

[21] K. Deb, A. Pratap, S. Agarwal, and T. Meyarivan, "A Fast and Elitist Multiobjective Genetic Algorithm: NSGA-II," *IEEE transactions on evolutionary computation*, vol. 6, no. 2, pp. 182–197, 2002.

[22] H. Akasaka, H. Nimiya, K. Soga, S. Matsumoto, K. Emura, N. Miki, E. Emura, and K. Takemasa, "Development of Expanded AMeDAS Weather Data for Building Energy Calculation in Japan," *ASHRAE Transactions*, vol. 106, pp. 455–465, 2000.